Rare Metal Materials and Engineering
Volume 50, Issue 9, September 2021
Available online at www.rmme.ac.cn

Science Press

Cite this article as: Lei Sheng, Liu Yafeng, Li Shuai, et al. Magnetic and Electrochemical Properties of FeCoCrNiZr$_x$ High-Entropy Alloys[J]. Rare Metal Materials and Engineering, 2021, 50(09): 3050-3055.

ARTICLE

Magnetic and Electrochemical Properties of FeCoCrNiZr$_x$ High-Entropy Alloys

Lei Sheng[1,2], Liu Yafeng[1], Li Shuai[1], Zhang Zhengbin[2], Hu Shanshan[1], Sun Xu[1]

[1] School of Mechanical and Electrical Engineering, Anhui Jianzhu University, Hefei 230601, China; [2] Key Laboratory of Intelligent Manufacturing of Construction Machinery, Hefei 230601, China

Abstract: FeCoCrNiZr$_x$ (x=0.5, 0.75, 1) high-entropy alloys with different Zr contents were prepared by vacuum arc melting. The effects of Zr content on the microstructure, magnetic properties, and electrochemical corrosion properties of the alloys were studied. X-ray diffraction, scanning electron microscope, vibration sample magnetometer, and electrochemical workstation were used to study the magnetic property and electrochemical corrosion ability of FeCoCrNiZr$_x$ alloys. Results show that FeCoCrNiZr$_x$ alloy has typical eutectic structure, consisting of face-centered cubic solid solution and C15 Laves phase. With the increase of Zr content, the hardness of the alloy increases at first and then decreases. However, according to the synthesized static hysteresis curves, FeCoCrNiZr$_{0.5}$ alloy shows a mixture characteristic of paramagnetism and ferromagnetism, FeCoCrNiZr$_{0.75}$ alloy has paramagnetic behavior, and FeCoCrNiZr$_1$ alloy has typical ferromagnetism. Meanwhile, the FeCoCrNiZr$_x$ alloy undergoes activation-passivation transition in 3.5wt% NaCl solution. When the content of Zr is 0.75at%, the polarization resistance of the alloy has the maximum impedance capacitance radius, and the corrosion resistance of the passive film is the strongest.

Key words: corrosion resistance; hardness; high-entropy alloy; magnetic property; microstructure

FeCoCrNi high-entropy alloy is one of the most stable alloys, which easily forms a solid solution with simple structures and has excellent plasticity and toughness. Chen[1] prepared AlCoCrFeNiZr$_x$ high-entropy alloys and analyzed their microstructure and mechanical properties. Results show that the alloys present two types of microstructures and Zr addition significantly improves the mechanical properties. When the Zr content is greater than 0.1at%, the fracture strength and plastic strain of the alloy are decreased significantly, but the yield strength is increased with further increasing the Zr content. CoCrFeNiZr$_x$ alloys with different Zr contents were prepared by Huo[2]. Typical eutectic structures are found in the alloys which are composed of face-centered cubic (fcc) solid solution and lamellar C15 Laves phase. The crystal orientation relationship between the two phases is determined. When the volume fraction of the hard C15 Laves phase increases, the strength of the alloy increases, but the alloy becomes more brittle at room temperature. The fracture process changes from ductile interlamellar fracture to brittle transduction fracture. Many studies have focused on the microstructure and mechanical properties of FeCoCrNiZr$_x$ alloys, but only a few studies have reported their functional properties (magnetization, magnetocaloric effect, resistance, etc)[3].

Zr is an important element in alloying with transition elements and has strong corrosion resistance. The crystal structure of Zr at room temperature is close-packed hexagonal. Under high-temperature conditions, the crystal structure transforms into body-centered cubic. Zr has a larger atomic radius and produces larger lattice distortion during the alloying procedure with other transition elements of Co, Cr, Fe, and Ni[4,5]. The mixing enthalpy of these elements is smaller than that of Al element, showing a strong tendency to form intermetallic compounds[6]. Zr is the key element to form Laves phase. The Laves phases, such as Co_2Zr, Cr_2Zr, and Fe_2Zr, all have C15 structure, which have excellent high-temperature oxidation resistance, alloy strength, and hot corrosion resistance. The FeCoCrNiZr$_x$ (x=0.5, 0.75, 1) high-

Received date: February 01, 2021
Foundation item: Natural Science Foundation of the Higher Education Institutions of Anhui Province, China (KJ2020ZD42)
Corresponding author: Lei Sheng, Ph. D., Professor, School of Mechanical and Electrical Engineering, Anhui Jianzhu University, Hefei 230601 P. R. China, E-mail: leish1964@vip.126.com

entropy alloys with different Zr contents were fabricated in this research to examine the effect of different Zr contents on the structure, magnetic properties, and electrochemical corrosion ability of the alloy system. The results also provide a good application basis for $FeCoCrNiZr_x$ (x=0.5, 0.75, 1) high-entropy alloys in the fields of magnetic components and microelectronic equipment.

1 Experiment

Fe, Co, Cr, Ni, and Zr (purity>99.9wt%) were smelted by arc on water-cooled plates in titanium-aspirated Ar gas. Table 1 shows the atomic radius and binary mixing enthalpy of each element. $FeCoCrNiZr_x$ high-entropy alloys with x=0.5, 0.75, 1 (at%) were prepared. The arc-melted ingot was remelted at least five times to ensure the uniformity of composition. After natural cooling, the ingot was cut into the specimen of 10×10×10 mm^3 in dimension by wire cutting.

The composition characteristic of specimens was analyzed by X-ray diffraction (XRD). The hardness was measured on the mirror surface of specimen by Wilson Hardness 401MVD microhardness tester. Four measured points were spaced 5 mm apart on the specimen surface, and the average hardness value was calculated. The surface morphology was observed using a scanning electron microscope (SEM). The magnetic properties of $FeCoCrNiZr_x$ high-entropy alloys were measured using a PPMSECII-97 integrated physical measurement system. The electrochemical corrosion properties of the alloys were measured using Autolab electrochemical workstation.

2 Results and Discussion

2.1 XRD analysis

Fig. 1 shows the XRD patterns of $FeCoCrNiZr_x$ (x=0.5, 0.75, 1) high-entropy alloys. The main phase is the fcc solid solution with γ-Fe structure. The fcc solid solution is an alloy consisting of Co, Cr, Fe, and Ni without Zr element. When the Zr content increases, the strongest peak moves to the left, indicating that the lattice constant of the cubic solid solution increases. In addition to the shift of diffraction peak of the cubic solid solution phase caused by the dissolution of Zr element into the FeCoCrNi system, some new corresponding diffraction peaks are observed[7]. When the Zr content is greater than 0.5at%, the reflection peak corresponding to the Laves phase of C15 structure appears, which is determined as ZrM_2 (M=Co or Ni).

Table 1 Atomic radius and binary mixing enthalpy of different elements

Element	Atomic radius/pm	Binary mixing enthalpy/kJ·mol^{-1}				
		Co	Cr	Fe	Ni	Zr
Co	126	-	−4	−1	0	−41
Cr	127	−4	-	−1	−7	−12
Fe	127	−1	−1	-	−2	−25
Ni	124	0	−7	−2	-	−49
Zr	160	−41	−12	−25	−49	-

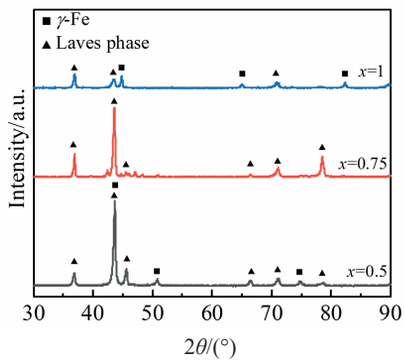

Fig.1 XRD patterns of $FeCoCrNiZr_x$ (x=0.5, 0.75, 1) alloys

The binary mixing enthalpy of Zr and other elements is relatively small, compared to that of Ni element. For example, the binary mixing enthalpy of Co-Zr and Ni-Zr is -41 and -49 kJ/mol, respectively. Moreover, when the atomic radius difference in the alloy is small, the simple solid-solution phase is more likely to form in the alloy[8]. As shown in Fig. 1, the increase of Zr content leads to a significant decrease in the mass fraction of fcc phase. In the $FeCoCrNiZr_{0.5}$ alloy, the Laves phase has the same strength as the fcc solid-solution phase does, indicating that the main phase is still a mixture of cubic solid solution[9]. The further increase of Zr content causes a decrease in the relative strength of the diffraction peak of fcc solid solution, whereas the relative strength of diffraction peak of the Laves phase increases, indicating that the volume fraction of the Laves phases is increased with the increase of Zr content.

2.2 Microstructure

Fig. 2 shows that $FeCoCrNiZr_x$ (x=0.5, 0.75, 1) alloys present a typical lamellar structure of eutectic alloy. Dark dendritic crystals of 10~100 μm in size are abundant in the $FeCoCrNiZr_{0.5}$ alloy. Some dark dendrites remain in the $FeCoCrNiZr_{0.75}$ alloy, but their amount significantly reduces. No dark dendritic crystals are found in the $FeCoCrNiZr_1$ alloy. During an eutectic reaction, the Laves phase and fcc solid solution form a small coupled lamellar layer[10]. Because only the two phases (ignoring the trace phases) are detected by XRD, the dark dendritic crystals and dark lamellar layers in the eutectic tissues belong to the same phase[11].

For $FeCoCrNiZr_x$ alloys with Zr content greater than 0.5at%, the Laves phases are observed at the grain boundary of fcc phase. The morphology of fcc phase is dendritic, and the Laves phase is the main phase[12]. When the Zr content increases, the volume fraction of the Laves phase also increases obviously. For the areas without Laves phase, the structure consists of periodic light and dark phases. The width of the periodic tissue is significantly larger, especially near the interface[13]. The further increase in Zr content causes grain refinement of the surrounding tissues again. It is difficult to detect the Zr element in the region without Laves phase. The dark phase without Laves phase is rich in Ni, while the light phase is rich in Fe, Cr, and Co evenly[14]. For the regions with

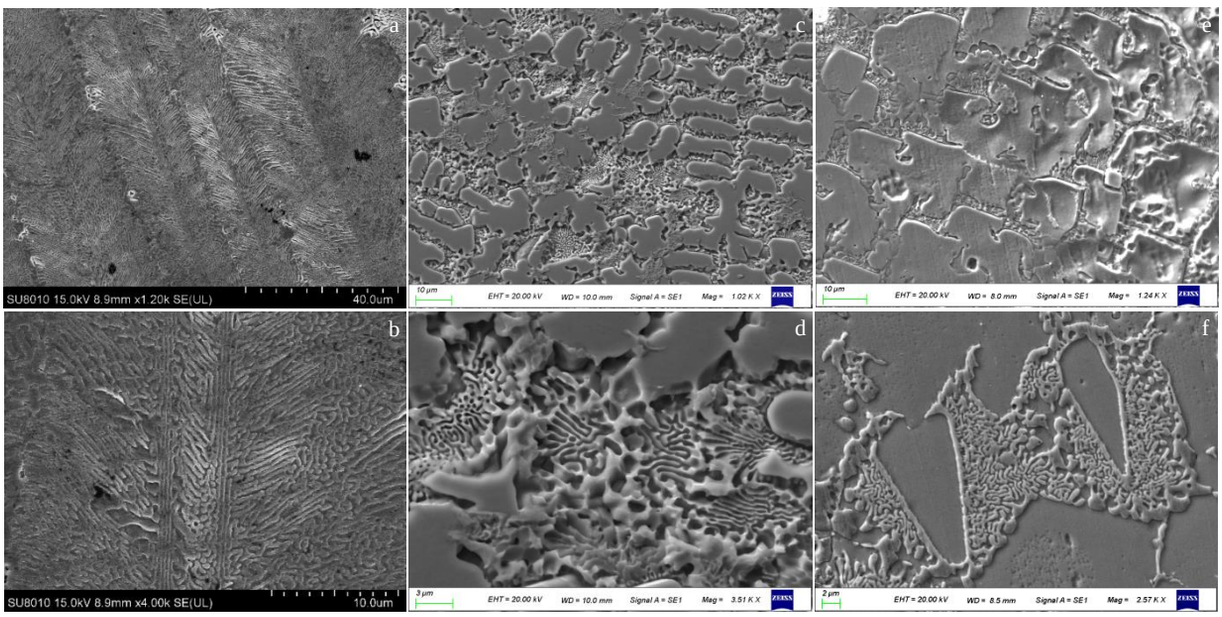

Fig.2 SEM images of $CoCrFeNiZr_x$ alloys: (a, b) $CoCrFeNiZr_{0.5}$, (c, d) $CoCrFeNiZr_{0.75}$, and (e, f) $CoCrFeNiZr_1$

Laves phase, the structure shows a mixed characteristic of fcc and Laves phases. This is due to the large lattice strain caused by the huge difference in the atomic size[15].

2.3 Hardness

Table 2 shows the hardness test results. For $FeCoCrNiZr_x$ (x =0.5, 0.75, 1) alloys, $CoCrFeNiZr_{0.75}$ alloy has the highest hardness with an average value of 5401 MPa. When Zr content is less than 0.75at%, the hardness of $FeCoCrNiZr_x$ high-entropy alloys shows an upward trend with the increase of Zr content. When Zr content exceeds 0.75at%, the hardness decreases. When the Zr content increases, the lattice constant of fcc phase in the alloy increases significantly. Zr addition causes an obvious lattice distortion effect, which increases the strength and hardness of the alloys. Therefore, the hardness of $FeCoCrNiZr_{0.75}$ alloy is higher than that of $FeCoCrNiZr_{0.5}$ alloy[16]. When the Zr content is 1at%, the hardness decreases to some extent probably due to the precipitation of γ-Fe in the phase[17].

2.4 Magnetic properties

Fig.3a and 3b show the hysteresis curves of $FeCoCrNiZr_x$ (x =0.5, 0.75, 1) alloys at room temperature. According to the static hysteresis curves, $FeCoCrNiZr_{0.5}$ alloy exhibits a mixture characteristic of paramagnetism and ferromagnetism, and $FeCoCrNiZr_{0.75}$ alloy exhibits the paramagnetic behavior. The saturation magnetization value of $FeCoCrNiZr_1$ alloy increases significantly. $FeCoCrNiZr_1$ shows the typical ferromagnetism characteristic[18] with a small coercive force H_c (1115.1986 A/m) and a large saturation magnetization M_s (8.5625 A·m^2/kg), indicating the soft magnetic properties. As the hysteresis curves of $FeCoCrNiZr_x$ alloys shown in Fig.4a

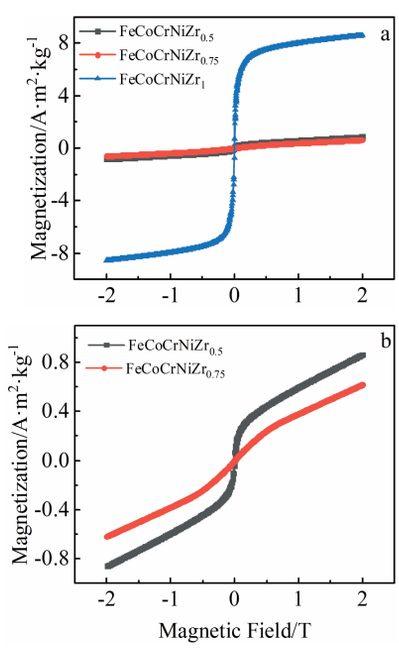

Fig.3 Hysteresis curves of $FeCoCrNiZr_x$ (x=0.5, 0.75, 1) alloys: (a) magnetization of -10~10 A·m^2/kg and (b) magnetization of -1.0~1 A·m^2/kg

Table 2 Hardness $HV_{0.2}$ of $FeCoCrNiZr_x$ (x=0.5, 0.75, 1) alloys (MPa)

No.	$FeCoCrNiZr_{0.5}$	$FeCoCrNiZr_{0.75}$	$FeCoCrNiZr_1$
1	3997	5342	4985
2	3786	5439	5303
3	3986	5285	5484
4	4118	5522	4956
5	4192	5419	5315
Average	4016	5401	5209

and 4b, only $FeCoCrNiZr_{0.5}$ alloy shows a relatively large hysteresis. The hysteresis area of $FeCoCrNiZr_{0.75}$ and $FeCoCrNiZr_1$ is small, and is basically zero for $FeCoCrNiZr_{0.75}$ alloy.

The existence of paramagnetic element Zr and antiferromagnetic element Cr in $FeCoCrNiZr_x$ high-entropy alloys has a great influence on the ferromagnetic elements (Fe, Co, and Ni). When the content of the diamagnetic elements and paramagnetic elements is large, the saturation magnetization value decreases, and the behavior of the alloy changes from ferromagnetic to paramagnetic[19,20]. Combined with the XRD analysis, the content of Laves phase in the physical phase decreases when the Zr content is 1at%, and the diffraction peak intensity suggests that γ-Fe phase is the basic phase. When the γ-Fe phase in the alloy becomes the main phase, the hardness decreases, but the paramagnetism of the $FeCoCrNiZr_1$ alloy is transformed into ferromagnetism[21,22]. When the Zr content is 0.5at%, the Laves phase is dominant in the alloy, and γ-Fe phase also exists in the alloy, so the composite alloy mainly shows a mixture characteristic of paramagnetism and ferromagnetism with a large hysteresis area. However, when the Zr content is 0.75at%, only the Laves phase is found in the physical phase, and the presence of the γ-Fe phase cannot be detected. The $FeCoCrNiZr_{0.75}$ alloy shows the most significant paramagnetic phenomenon, and the hysteresis area is basically zero. The analysis shows that the relative volume fraction of the synthesized fcc phase changes significantly. When the Zr content changes, the lattice parameters of the fcc phase change slightly, indicating that the increase of saturation magnetization value and the improvement of magnetic properties of the high-entropy alloys are related to the change in the relative volume fraction of the fcc phase.

2.5 Electrochemical corrosion behavior

Fig. 5 shows the potentiodynamic polarization curves of $FeCoCrNiZr_x$ high-entropy alloys in 3.5wt% NaCl solution at room temperature. Table 3 shows the electrochemical parameters of the alloy in the 3.5wt% NaCl solution. The corrosion current density (I_{corr}) was obtained from the intersection of the corrosion potential (E_{corr}) and the tangent line in the Tafel region of the cathode[23]. Obvious passivation zones are observed in $FeCoCrNiZr_x$ alloys, and the transition zone between the activation and passivation regions occurs during the transition from the Tafel region to the passivation region. During the electrochemical experiment, the alloys undergo an activation-passivation transition. $FeCoCrNiZr_{0.75}$ high-entropy alloy has the highest corrosion potential and the lowest corrosion current density, indicating the lowest corrosion rate. The wider the passivation area, the stronger the ability to inhibit the corrosion reaction. Moreover, the $FeCoCrNiZr_{0.75}$ alloy is mainly composed of Laves phase, and Zr compounds present a higher tendency to form a passivating film[24,25].

Fig.6 shows the semicircular Nyquist plots of $FeCoCrNiZr_x$ high-entropy alloys, suggesting the charge transfer mechanism. The larger the radius of the impedance capacitance, the stronger the corrosion resistance of high-entropy alloys[26,27]. The impedance capacitor of $FeCoCrNiZr_{0.75}$ alloy has the largest radius, i. e., the passivation film of $FeCoCrNiZr_{0.75}$ alloy has the strongest corrosion resistance,

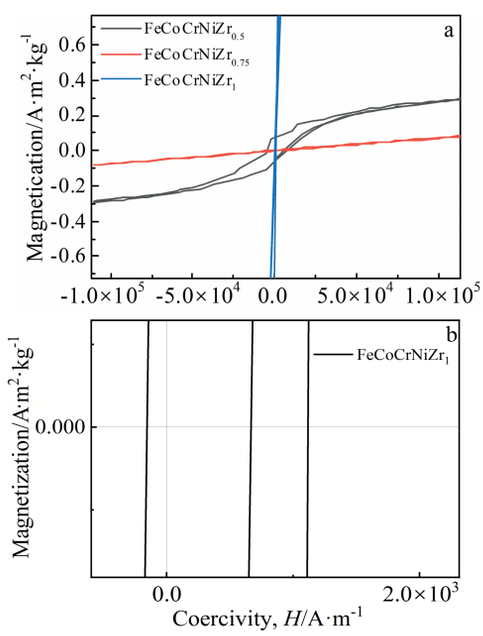

Fig.4 Hysteretic regions of $FeCoCrNiZr_x$ (x=0.5, 0.75, 1) alloys: (a) coercivity of -1.0×10^5~1.0×10^5 A/m and (b) coercivity of 0.0~2.0×10^3 A/m

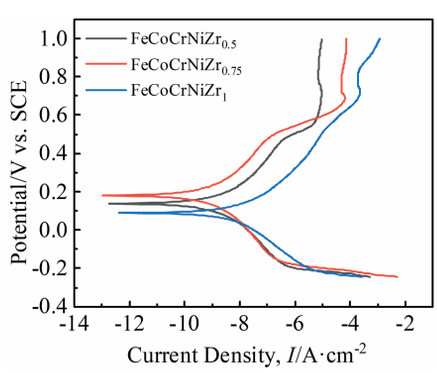

Fig.5 Potentiodynamic polarization curves of $FeCoCrNiZr_x$ (x=0.5, 0.75, 1) alloys

Table 3 Electrochemical parameters of $FeCoCrNiZr_x$ alloys in 3.5wt% NaCl solution

Alloy	Corrosion potential, E_{corr}/V	Corrosion current density, I_{corr}/A·cm^{-2}
$FeCoCrNiZr_{0.5}$	0.139	-9.633
$FeCoCrNiZr_{0.75}$	0.181	-10.059
$FeCoCrNiZr_1$	0.089	-8.909

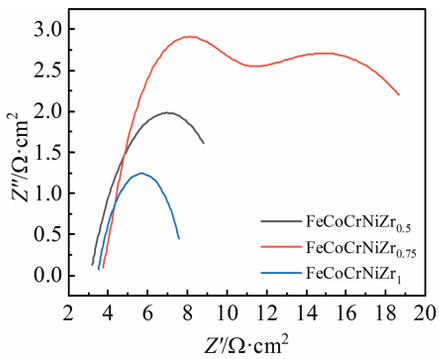

Fig.6 Nyquist plots of FeCoCrNiZr$_x$ (x=0.5, 0.75, 1) alloys

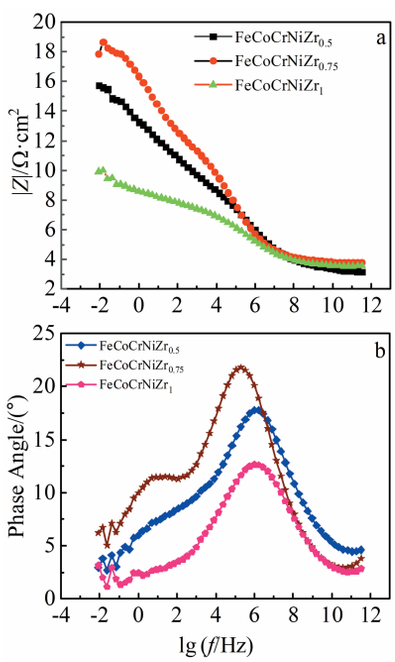

Fig.7 Bode diagrams of FeCoCrNiZr$_x$ (x=0.5, 0.75, 1) alloys: (a) impedance modulus and (b) phase angle

which is consistent with the aforementioned results[28].

Fig. 7 shows the Bode diagrams of FeCoCrNiZr$_x$ alloys. Within the lower frequency range, FeCoCrNiZr$_{0.75}$ alloy has the highest complex impedance modulus, indicating the highest corrosion resistance of the passivation film. The phase angle diagram shows a significant difference in the performance of passivation film of FeCoCrNiZr$_x$ alloy[29]. The FeCoCrNiZr$_{0.75}$ high-entropy alloy has the largest phase angle of about 23° and two peaks, showing the best corrosion resistance. The peak phase angles of FeCoCrNiZr$_{0.5}$ and FeCoCrNiZr$_1$ alloys are 17° and 13°, respectively. The lower phase angle indicates a weakened protective ability of the passivation film.

3 Conclusions

1) FeCoCrNiZr$_x$ alloys mainly consist of face-centered cubic (fcc) solid solution, γ-Fe phase, and ZrM_2 (M=Co, Ni) with C15 Laves phase. The Zr addition increases the lattice constant of fcc solid solution. The microstructure of the eutectic alloy is the typical fine layer structure. When the Zr content and the relative volume fraction of the Laves phase increase, the hardness of the alloy firstly increases and then decreases.

2) With the increase of Zr content, the magnetic properties of FeCoCrNiZr$_x$ (x=0.5, 0.75, 1) alloys are gradually enhanced. FeCoCrNiZr$_1$ alloy has the best magnetism, and the saturation magnetization M_s and coercive force H_c are 8.5625 A·m^2/kg and 1115.1986 A/m, respectively.

3) FeCoCrNiZr$_{0.75}$ alloy has the highest corrosion potential and the lowest corrosion current density, i.e., FeCoCrNiZr$_{0.75}$ alloy has the best corrosion resistance. The Zr compounds form an excellent passivation film during the electrochemical corrosion and improve the corrosion resistance of the alloys.

References

1 Chen J, Niu P Y, Liu Y Z *et al. Materials & Design*[J], 2016, 94: 39

2 Huo W Y, Zhou H, Fang F *et al. Materials & Design*[J], 2017, 134: 226

3 Zhang H L, Zhang L, Liu X Y *et al*. *Entropy*[J], 2018, 20(11): 810

4 Qiu S, Zhang X C, Zhou J *et al. Journal of Alloys and Compounds*[J], 2020, 846: 156 321

5 Li M Y, Guo Y H, Wang H L *et al. Intermetallics*[J], 2020, 123: 106 819

6 Xie Hongbo, Liu Guizhong, Guo Jingjie. *Journal of Materials Engineering*[J], 2016, 44(6): 44 (in Chinese)

7 Feng X G, Zhang K F, Zheng Y G *et al*. *Nuclear Inst and Methods in Physics Research B*[J], 2019, 457: 56

8 Zhang Y, Zhou Y J, Lin J P *et al*. *Advance Engineering Materials* [J], 2008, 10(6): 534

9 Shuai C, Yong S, Duan Y H *et al*. *Journal of Alloys and Compounds*[J], 2015, 630: 202

10 Yurchenko N Y, Stepanov N D, Gridneva A O *et al*. *Journal of Alloys and Compounds*[J], 2018, 757: 403

11 Vrtnik S, Guo S, Sheikh S *et al*. *Intermetallics*[J], 2018, 93: 122

12 Tariq N H, Naeem M, Hasan B A *et al. Journal of Alloys and Compounds*[J], 2013, 556: 79

13 Tsai M H, Fan A C, Wang H A. *Journal of Alloys and Compounds*[J], 2017, 695: 1479

14 Fan A C, Li J H, Tsai M H. *Journal of Materials Research and Technology*[J], 2020, 9(5): 11 231

15 Krčmar M, Fu C L. *Intermetallics*[J], 2007, 15(1): 20

16 Feng X B, Fan S F, Meng F L *et al*. *Applied Nanoscience*[J], 2021, 11(3): 776

17 Dong Wanqing. *Thesis for Master*[D]. Yanshan: Yanshan University, 2020 (in Chinese)

18 Lei S, Sun J, Wu Y B *et al*. *Ordnance Material Science and Engineering*[J], 2019, 42(4): 72

19 Zhao C D, Li J S, Liu Y D *et al*. *Journal of Materials Science and Technology*[J], 2021, 73: 83
20 Yang Y, Feng Z Y, Zhang J M. *Applied Surface Science*[J], 2018, 457: 403
21 Yu P F, Zhang L J, Cheng H *et al*. *Intermetallics*[J], 2016, 70: 82
22 Li P P, Wang A D, Liu C T. *Journal of Alloys and Compounds*[J], 2017, 694: 55
23 Wang Q, Amar A, Jiang C *et al*. *Intermetallics*[J], 2020, 119: 106 727
24 Niu Z Z, Wang Y Z, Geng C *et al*. *Journal of Alloys and Compounds*[J], 2020, 820: 153 273
25 Bai Y K, Ling Y H, Lai W S *et al*. *Applied Surface Science*[J], 2016, 388: 212
26 Shang X L, Wang Z J, Wu Q F *et al*. *Acta Metallurgica Sinica* (*English Letters*)[J], 2019, 32(1): 41
27 Zhao Y, Wang M L, Cui H Z *et al*. *Journal of Alloys and Compounds*[J], 2019, 805: 585
28 Cai B X, Yang L. *Journal of Wuhan University of Technology* (*Materials Science*)[J], 2019, 34(4): 791
29 Yang Zhongbo, Cheng Zhuqing, Qiu Jun *et al*. *Rare Metal Materials and Engineering*[J], 2018, 47(3): 794

FeCoCrNiZr$_x$高熵合金的磁性和电化学性能

雷　声[1,2]，刘亚峰[1]，李　帅[1]，张正彬[2]，胡珊珊[1]，孙　旭[1]
(1. 安徽建筑大学 机械与电气工程学院，安徽 合肥 230601)
(2. 工程机械智能制造重点实验室，安徽 合肥 230601)

摘　要：采用真空电弧熔炼法制备了不同Zr含量的FeCoCrNiZr$_x$（x=0.5，0.75，1）高熵合金。研究了Zr含量对合金组织、磁性能和电化学腐蚀性能的影响。采用X射线衍射仪、扫描电镜、振动样品磁力计和电化学工作站对合金的磁性能和电化学腐蚀能力进行了研究。结果表明：FeCoCrNiZr$_x$合金具有典型的共晶组织，由面心立方固溶体和C15 Laves相组成。随着Zr含量的增加，合金硬度呈先增大后减小的趋势。根据合成的静态滞回曲线可以看出，FeCoCrNiZr$_{0.5}$合金具有顺磁性和铁磁性的混合型特征，FeCoCrNiZr$_{0.75}$合金表现为顺磁性，FeCoCrNiZr$_1$合金表现为典型的铁磁性。同时，FeCoCrNiZr$_x$合金在3.5%（质量分数）NaCl溶液中经历活化与钝化转变。当合金中的Zr含量为0.75%（原子分数）时，合金极化电阻具有最大的阻抗电容半径，钝化膜的耐腐蚀能力最强。

关键词：耐蚀性；硬度；高熵合金；磁性；微观结构

作者简介：雷　声，男，1964年生，博士，教授，安徽建筑大学机械与电气工程学院，安徽 合肥 230601，E-mail：leish1964@vip.126.com